THE ASTROPHYSICAL JOURNAL, 225:465–481, 1978 October 15

ULTRAVIOLET OBSERVATIONS OF COOL STARS. VII. LOCAL INTERSTELLAR HYDROGEN AND DEUTERIUM LYMAN-ALPHA

W. MCCLINTOCK* AND R. C. HENRY†
Physics Department, The Johns Hopkins University
J. L. LINSKY†‡
Joint Institute for Laboratory Astrophysics, National Bureau of Standards and University of Colorado
AND
H. W. MOOS†
Physics Department, The Johns Hopkins University
Received 1977 December 27; accepted 1978 April 25

ABSTRACT

We present and analyze high-resolution *Copernicus* observations of the interstellar hydrogen and deuterium Lα lines toward ϵ Eri (3.3 pc) and ϵ Ind (3.4 pc). We also reanalyze previous observations toward α Cen A (1.3 pc) and α Aur (14 pc). For these stars the hydrogen and deuterium interstellar parameters are derived independently, with no assumptions concerning the deuterium-to-hydrogen ratio. In all cases profile synthesis leads to a range of acceptable parameters, since very similar absorption profiles result from increasing the hydrogen density (n_H) while decreasing the Doppler dispersion parameter (b_H) and similarly for n_D and b_D. We conclude that all the stellar and solar system data are consistent with a homogeneous region within 3.5 pc of the Sun in which $n_H \approx 0.10$–0.15 cm^{-3} and in which the flow velocity is 22 km s^{-1} from the direction $\alpha = 252°$, $\delta = -15°$. Beyond 3.5 pc the density probably decreases as $n_H = 0.04$–0.05 cm^{-3} toward α Aur, but the flow vector is unchanged. There is no conclusive evidence that the deuterium-to-hydrogen ratio toward the four stars is significantly different from the value $1.8 \pm 0.4 \times 10^{-5}$ derived by York and Rogerson toward OB stars. We also conclude that the existence of a nearby interstellar cloud, which Vidal-Madjar *et al.* have proposed as approaching the solar system from 0.03 pc, is not supported by the data.

Subject headings: deuterium — interstellar: abundances — interstellar: matter — ultraviolet: spectra

I. INTRODUCTION

McClintock *et al.* (1976*a*, Paper V) reported a high-resolution *Copernicus* observation of the hydrogen Lα emission line of the nearby (3.3 pc) K2 dwarf ϵ Eri and from the observed interstellar absorption derived a value for the mean local interstellar hydrogen density of $n_H = 0.08 \pm 0.04$ cm^{-3}. This assumed a velocity dispersion parameter $b = 9$ km s^{-1}, corresponding to a temperature of 5000 K. Very low densities (≤ 0.01 cm^{-3}) were shown to be unlikely unless one permitted large b-values (> 14 km s^{-1}). In the observation reported in Paper V, the interstellar line was saturated and geocoronal emission contaminated one wing of the interstellar line. Since an unambiguous profile for the line could not be determined, the analysis was carried out with two different assumptions concerning what lay under the geocoronal emission. We have repeated the observation, this time choosing the time of observation such that the geocoronal emission lies in the center of the highly saturated core of the interstellar Lα absorption line. Thus both wings of the interstellar line are observed, and we find that profile 2 of Paper V is correct. The new observation also greatly improves the statistical reliability of the line profile.

In Paper V evidence was also given for the presence of interstellar deuterium Lα absorption in the blue wing of the stellar chromospheric Lα emission line. The improved accuracy of the present observation confirms the detection of this line. Since the deuterium line is on a completely different portion of the curve of growth (weak-to-saturated) compared with the hydrogen line, the two observations combine to give additional information concerning the density and temperature (or state of turbulence) of the local interstellar gas toward ϵ Eri.

We have also observed a second star, ϵ Ind. This K5 dwarf is 3.5 pc distant and lies in a direction ($l = 336°$, $b = -48°$) quite different from that of ϵ Eri ($l = 196°$, $b = -48°$). We again observed a

* Currently at the Joint Institute for Laboratory Astrophysics and the Laboratory for Atmospheric and Space Physics, University of Colorado.

† Guest Investigator with the Princeton University telescope on the *Copernicus* satellite, which is sponsored and operated by the National Aeronautics and Space Administration.

‡ Staff Member, Quantum Physics Division, National Bureau of Standards.

saturated interstellar hydrogen line and an interstellar deuterium Lα line. These observations have been previously presented by McClintock *et al.* (1976*b*).

Other analyses of interstellar hydrogen and deuterium Lα absorption in the line of sight toward nearby late-type stars include studies of α Aur and α Cen A (Dupree, Baliunas, and Shipman 1977). Since Dupree *et al.* suggest large variations in the local interstellar hydrogen density and in the deuterium-to-hydrogen (D/H) ratio, which as they point out would have important cosmological consequences if confirmed, we have reanalyzed these data using the same methods employed for ε Eri and ε Ind.

In § II we present, reduce, and analyze our high-resolution *Copernicus* spectra of ε Eri, and in § III we similarly treat our ε Ind data. Because the techniques used here differ from those of other authors, we have included a detailed description of our procedures. Section IV is our reanalysis of the *Copernicus* spectra of α Aur and α Cen A. Finally, in § V we compare our estimates of the local interstellar medium parameters with those obtained by other techniques, and we show that there is no compelling evidence for significant variations in the hydrogen density and D/H ratio in the local interstellar medium. On this basis we reject the hypothesis of an approaching local interstellar cloud proposed by Vidal-Madjar *et al.* (1978).

II. ε ERIDANI

a) Observations

In Paper IV (McClintock *et al.* 1975*a*) we presented *Copernicus* U2 (0.25 Å) observations of the Lα chromospheric emission line in ε Eri, the first observation of this line in a dwarf star other than the Sun. These low-resolution data indicated that the shape of the emission profile is similar to but slightly narrower than that of the solar Lα line and that the stellar surface flux on the day of observation was the same order of magnitude as the value for the quiet Sun. Unlike the solar profile, however, the observed intensity at line center is nearly zero. This dark central reversal is unlikely to be intrinsic to the emission from a dwarf-star chromosphere, because the line source function at small Lα line-center optical depths is $\sim n_e^{1/2} B_\nu(T)$, where n_e is the electron density and $B_\nu(T)$ the local Planck function. Unless n_e is at least two orders of magnitude lower than in the solar chromosphere at temperatures $\sim$20,000 K, the intrinsic stellar line should show either a small central depression as in the Sun or none at all. In fact, the extremely weak reversal that is present in the Ca II lines (Kelch 1978) suggests chromospheric densities larger than in the Sun. The dark central core of Lα must, therefore, be due to circumstellar or interstellar absorption. Since there is no evidence for circumstellar material around ε Eri or any other K dwarf, we assume that the dark core is entirely interstellar in origin.

In order to measure the column density of neutral hydrogen toward ε Eri, the Lα emission line was reobserved on 1975 January 15/16 (Paper V) and on 1975 September 1/2 (McClintock *et al.* 1976*b*), using the U1 detector (0.05 Å resolution).

i) *1975 January Observation*

In Paper V the 1975 January data were presented as an average profile, after subtraction of a background (due primarily to energetic particles) estimated from the "standard table of backgrounds" described by McClintock *et al.* (1975*b*, Paper III). Alternative methods of data processing and of background subtraction give substantial additional insight into the meaning and value of the data. The solid line in Figure 1 is an average of the 1975 January scans (48) of ε Eri, with particle backgrounds removed using the U2 detector as a real-time background monitor.[1] A typical rms error bar is shown above the plot. We have deleted five spectral steps that are dominated by geocoronal Lα emission and also two partially contaminated steps. The ordinate is average U1 counts per 14 s, and the abscissa is vacuum wavelength in the stellar rest frame.

The dashed line in Figure 1 is an average of the same data, from which particle backgrounds have been subtracted using the standard table of backgrounds as in Paper V. The overall agreement between the two subtraction techniques is of lesser quality than that found for the September 1975 observation, described below. The discrepancy for five points near λ1215.3 is particularly severe. The situation was not substantially improved when restricted averages of the data were made by deleting (*a*) scans with particularly large background count rates, (*b*) scans interrupted by occultation of the star by the Earth, (*c*) the first 24 scans, or (*d*) the last 24 scans. We also separately co-added the two backgrounds as a function of wavelength, to search for some obvious discrepancy. We saw a rather sharp decline in the standard table backgrounds near λ1215.3, but the U2 backgrounds showed a somewhat smaller rise. Although we believe that this discrepancy should not affect the identification of the deuterium Lα absorption line near λ1215.34,

[1] The scale factor used to convert U2 backgrounds into expected U1 counts was 1.32 U2 counts = 1.0 U1 counts. This factor was determined by comparing U1 and U2 count rates for sets of several hundred scans in a spectral range where no stellar emission was detected (McClintock 1977). We found the scale factor to vary by a few percent for the different data sets. In order to test the sensitivity of the estimated backgrounds to our choice of scale factor, the data were also reduced with scale factors ±20% different. In these tests the only observable effect was a shift in the zero level, but there was no change in the spectrum shape. We therefore adopted the value 1.3 but determined the zero level for each observation from the saturated core of the interstellar hydrogen Lα line. The errors for this method were computed from the rms errors of the individual scans about the mean of 48 scans. In general, these errors usually agree within a few percent with those computed from Poisson distributions characterizing both the stellar signal and the background. Also, the random errors in the background tables are comparable to those for the U2 real-time monitor when 20 or more scans are co-added. As discussed in Gerola *et al.* (1977), electronic pickup in the U2 monitor channel has been avoided by our choice of observing sequence.

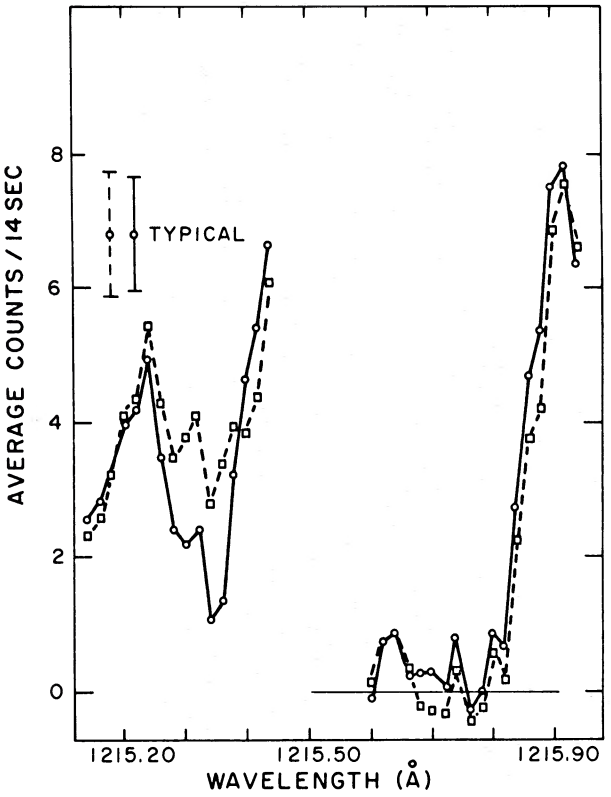

FIG. 1.—The solid line is the high-resolution observation of Lα in ε Eri obtained on 1975 January 15/16 after subtraction of a background using the real-time monitor. The dashed line shows the same Lα data but after subtraction of a background estimated from the "standard table." Points contaminated by geocoronal Lα emission have been deleted; ±1 σ errors in the mean for each data point are noted by the error bars.

it does imply uncertainty in the measurement of the position of line center and also produces a large uncertainty in the equivalent width (see below). An additional cause for concern is the fact that the deuterium profile is much broader than is expected for an interstellar line. One could argue that the instrumental profile, in practice, is broader than 0.05 Å because of guidance errors and/or temperature gradients in the spectrometer during repeated observations of a faint red star from orbit to orbit. Although the pointing accuracy for these data is of lesser quality than for the other observations reported here, test degradation of the resolution of simple models described below demonstrated that guidance errors could account for only a small fraction (20% or less) of the apparent broadening. Furthermore, a check of spectrometer thermistors for a time period from 12 hours before this observation until its end showed no evidence for temperature changes.

The wavelength scale in Figure 1 has been corrected by +0.03 Å (7.4 km s^{-1}) using the geocoronal Lα line as a wavelength standard. The uncertainty in the wavelength scale is ±7.5 km s^{-1}. Although the position of the geocoronal Lα can be determined to 0.01 Å (½ step), changes in spacecraft pointing may cause shifts of up to ±7 km s^{-1} between the wavelength scale for a stellar source and the wavelength calibration determined from an extended source. The applied correction is in agreement with the value +8.1 km s^{-1} calculated from the relationship between wavelength scale and spectrometer temperature given by Shull and York (1977).

ii) *1975 September Observation*

The solid line in Figure 2 is an average of 48 scans made during the 1975 September observation of ε Eri with particle backgrounds removed using the U2 detector as a real-time background monitor, while the dashed line is an average of the data for which particle backgrounds were estimated from the standard table. In contrast to the 1975 January data, the two methods of background subtraction agree well everywhere.

The wavelength scale in Figure 2 was corrected by +0.013 Å (3.3 km s^{-1}) using the geocoronal Lα line as a wavelength standard. This correction is in agreement with the value +4.1 km s^{-1} calculated from the relation given by Shull and York.

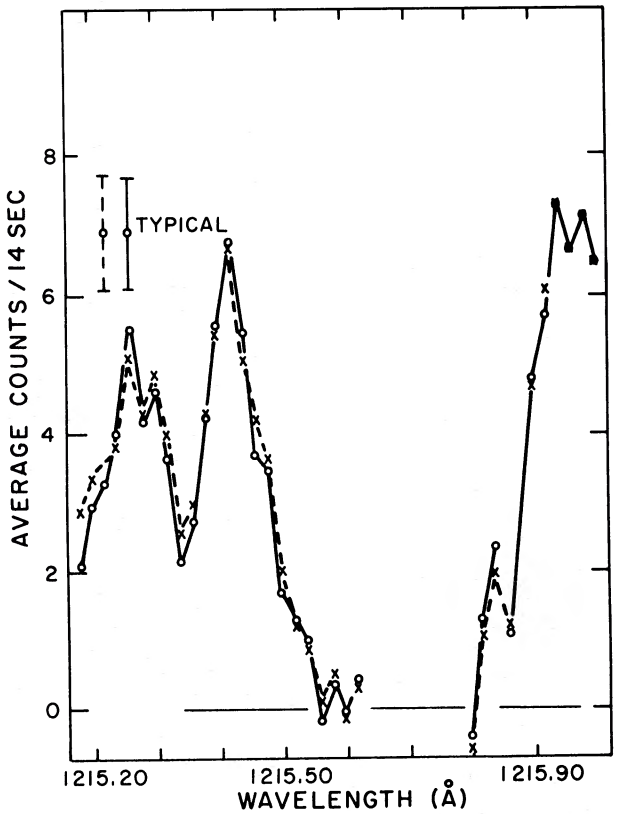

FIG. 2.—The high-resolution observation of Lα in ε Eri obtained on 1975 September 1/2. The solid and dashed lines show the results of subtracting backgrounds using the real-time monitor and the "standard table," respectively. See also Fig. 1.

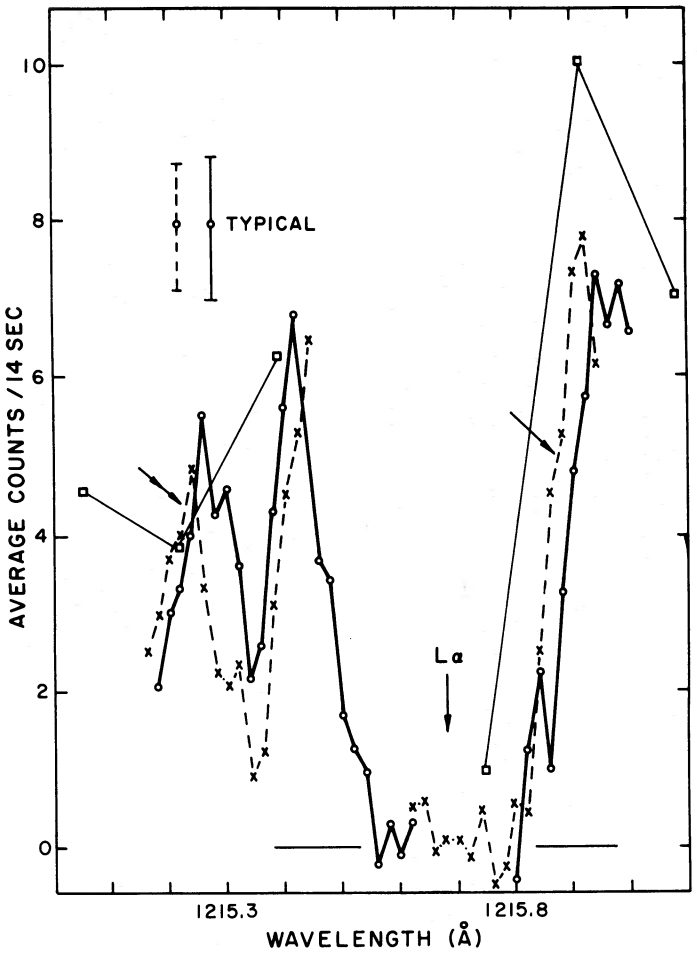

FIG. 3.—The solid line connecting circles and the dashed line are the two high-resolution observations of Lα in ε Eri. In each case, the data were corrected using the real-time monitor and the wavelength scales were determined using geocoronal Lα emission as a wavelength standard. The thin solid line connecting squares is the low-resolution (U2) observation described in Paper IV.

iii) *Intercomparison of ε Eridani Observations*

Figure 3 is a comparison of the two high-resolution observations which were reduced using the real-time backgrounds. The shift in the long-wavelength wing of the interstellar hydrogen profile, marked by the single-headed arrow, and the short-wavelength edge of the stellar profile, marked by the double-headed arrow, are less than the stated uncertainty of ± 7.5 km s^{-1} (0.03 Å) for determining the wavelength scales from the position of the terrestrial Lα emission. Rather than risk an overinterpretation of the data by aligning spectral features, we adopt the wavelength scale shown in Figure 3 for analyzing both observations. The thin solid line connecting squares represents the U2 data of Paper IV. The low-resolution and high-resolution observations are consistent, except for a possible small relative shift in the high-resolution and low-resolution wavelength scales.

b) Analysis of the ε Eridani Observations

In our analysis of the absorption-line data for nearby stars, we assume that interstellar material along the line of sight may be characterized by a single average density and that the velocity distribution of the absorbers is Maxwellian. This is reasonable if the local interstellar medium (LISM) is composed of a single neutral component and the line of sight intercepts no clouds, or if the LISM is hot and mostly ionized and the line of sight intercepts a single cloud. Significant errors in density determinations will result if a single Gaussian curve of growth is assumed for what is in fact a multicomponent line of sight (Nachman and Hobbs 1973; Shull and York 1977). We also assume that hot low-density neutral hydrogen created by charge exchange between solar wind protons and the very local interstellar hydrogen will have a negligible effect on the column density toward nearby stars.

Three parameters may be obtained from the analysis of absorption lines under our assumptions—the bulk line-of-sight velocity, the average density, and the Doppler dispersion parameter. The bulk velocity may be determined by inspection of the data, but the other two parameters must be derived by fitting profiles of

absorption lines to the observations, or by comparing measured and theoretical equivalent widths. We follow the treatment of interstellar absorption-line profiles given by Münch (1968). The optical depth may be written in the form

$$\tau(\lambda) \propto nLH(a, u), \quad (1)$$

where n is the average interstellar density of the species, L is the path length, $H(a, u)$ is the Voigt function, a is the damping constant, $u = [\lambda - \lambda_0(1 + V_0/c)]/b$, and b is $\sqrt{2}$ times the Doppler dispersion along the line of sight in wavelength units. Here, V_0 is the mean line-of-sight velocity of the interstellar matter.

When the total column density of hydrogen $N_H \lesssim 10^{18}$ atoms cm^{-2}, the wings of the Lα profiles ($\Delta\lambda \gtrsim 0.2$ Å) are determined primarily by the column density while the width of the saturated core of the line is dominated by the choice of b_H. For $N_H \gtrsim 1.6 \times 10^{18}$, pure damping and Voigt profiles are nearly indistinguishable for the range of b-values considered here.

The isotopic shift in laboratory wavelength for deuterium Lα relative to hydrogen Lα is -0.332 Å; so long as the total column density of hydrogen is not too great, deuterium Lα should be readily discerned in the short-wavelength wing of the hydrogen line. Examples of composite deuterium-hydrogen Lα absorption profiles are shown in Figure 4 for hydrogen densities of 0.06, 0.10, and 0.14 cm^{-3} and a column length of 3.3 pc. All profiles were convolved with a triangular profile having FWHM = 0.05 Å. We assumed a ratio of deuterium to hydrogen $n_D/n_H = 1.8 \times 10^{-5}$ and a ratio of the Doppler dispersion parameters $b_D/b_H = 1/\sqrt{2}$. Curve-of-growth calculations indicate that, for $N_D = 1.8 \times 10^{13}$ (corresponding to $n_H = 0.1$ cm^{-3}, $n_D/n_H = 1.8 \times 10^{-5}$, and $L = 3.3$ pc), the deuterium line is on the flat part of the curve of growth. Therefore, deuterium column densities derived from measured equivalent widths of the deuterium Lα line depend sensitively on the choice of Doppler dispersion parameter b_D.

i) *Line-of-Sight Bulk Velocities*

For the September observation, we measured a hydrogen absorption line center of 1215.68 ± 0.01 Å and a deuterium absorption line center of 1215.34 ± 0.01 Å, in the rest frame of the star (heliocentric radial velocity, +15.4 km s^{-1}).[2] These measurements are consistent with an isotopic wavelength shift of -0.332 Å. The inferred heliocentric line-of-sight velocity component of atomic hydrogen and deuterium is therefore 17.9 ± 7.5 km s^{-1}. The interstellar hydrogen line in the January data provides only broad limits to the bulk velocity, because the short-wavelength wing of the main absorption feature is contaminated by geocoronal Lα emission. Although the January deuterium line profile is of lower quality as a consequence of uncertainties in the background subtraction, the line-center wavelength 1215.33 ± 0.02 Å

[2] This is the mean of the four most recent determinations cited by Abt and Biggs (1972).

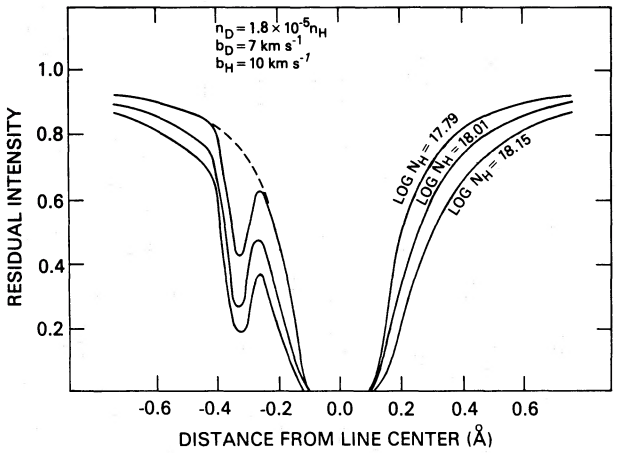

FIG. 4.—The solid lines are examples of composite hydrogen Lα and deuterium Lα absorption profiles for a path length of 3.3 pc and densities of 0.06 cm^{-3}, 0.10 cm^{-3}, and 0.14 cm^{-3}, corresponding to the three hydrogen column densities cited. In each case, the deuterium-to-hydrogen ratio is fixed at $D/H \equiv n_D/n_H = 1.8 \times 10^{-5}$. The dashed line indicates the hydrogen absorption profile for no deuterium.

obtained by measuring the midpoint of the profile at half-intensity is consistent with the value obtained for the September observation.

ii) *Analysis of the Deuterium Line*

For the September observation of ϵ Eri, the measured deuterium-line equivalent width is W_λ(September) = 58 ± 14 mÅ. We obtain W_λ(January) = 94 ± 15 mÅ if the real-time monitor is used to estimate the particle backgrounds (*solid line* in Fig. 2) or W_λ(January) = 72 ± 15 mÅ if the standard table is used to estimate the particle backgrounds (*dashed line* in Fig. 2). Although the co-added U2 backgrounds are somewhat better behaved than the standard table backgrounds (§ II*a*[i]), we adopt the mean of the two values, W_λ(January) = 83 ± 21 mÅ. For $b_D = 7$ km s^{-1} (see Table 1), W_λ(September) = 58 ± 14 mÅ leads to $n_D = 2.0(+1.0, -0.8) \times 10^{-6}$ cm^{-3} and W_λ(January) = 83 ± 21 mÅ leads to $n_D = 5.0(+5.0, -2.3) \times 10^{-6}$ cm^{-3}.

iii) *Analysis of the Hydrogen Absorption Profile*

Since the intrinsic stellar Lα emission profile is unknown, it is not possible to measure the equivalent width of the hydrogen absorption line. Instead, we estimate n_H by constructing simple models for the stellar emission line and the interstellar absorption line and by comparing the results with observed profiles.

From examining low-resolution observations, we assume that the intrinsic stellar emission line $I_0(\lambda)$ has the general shape observed for the solar profile (Bruner and Rense 1969) but we allow for various possible amounts of self-absorption. We then construct a grid of models using the following procedure,

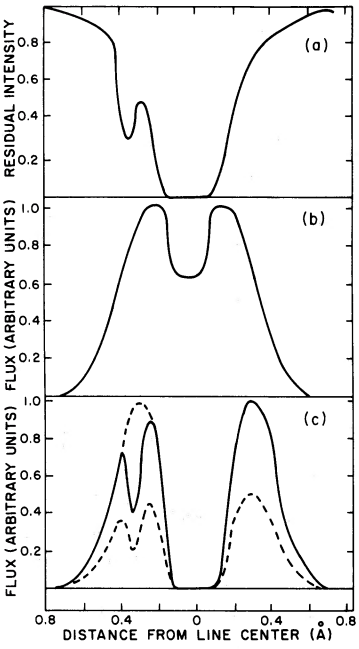

FIG. 5.—An example of the model-fitting procedure used to determine interstellar parameters. (*a*) A composite hydrogen-deuterium absorption profile. (*b*) An assumed intrinsic stellar Lα profile. (*c*) The lower dashed line shows the observed profile which results from the interstellar absorption in Fig. 5*a* acting on the intrinsic profile; the solid line is identical to the dashed line, except that the profile is normalized to unit height; the upper dashed line indicates the profile which would be observed in the absence of deuterium absorption.

illustrated in Figure 5 and described in further detail by McClintock (1977):

1. We choose an emission-line half-width, and a shape and depth of the self-reversal for the stellar profile. From the parameters we compute $I_0(\lambda)$—for example, the profile with a FWHM = 0.8 Å and a 35% self-reversed core illustrated in Figure 5*b*.

2. We then independently choose n_H and n_D, and the Doppler dispersion parameters b_H and b_D. Voigt profiles are next computed and convolved with a triangular instrumental profile having FWHM = 0.05 Å. Figure 5*a* is an example of an absorption profile $\exp[-\tau(\lambda)]$ for $n_H = 0.1$ cm^{-3}, $b_H = 12$ km s^{-1}, $n_D/n_H = 1.8 \times 10^{-5}$, and $b_D/b_H = 1/\sqrt{2}$. In all cases, the hydrogen and deuterium absorption profiles are *independently fitted* to the data, without assuming any *a priori* relations between n_H and n_D and between b_H and b_D.

3. We next combine the two profiles to form the observed profile, as illustrated by the dashed profile in Figure 5*c*.

4. We finally normalize the resulting profile to unit height for comparison with the data. The example model profile is shown as the solid line in Figure 5*c*. Note that the deuterium-line equivalent width can be accurately measured only by comparison with a computed profile assuming no deuterium (*dashed line* in the upper part of Fig. 5*c*). In principle, the stellar profile should be multiplied by the interstellar Voigt profile before convolution with the instrumental profile. However, detailed testing showed that none of our results are changed by using the order outlined above. If one wishes to estimate the intrinsic stellar profile, however, multiplication by the Voigt profile first is important.

The solid line in Figure 6*a* shows the range of n_H and b_H permitted by the profile fit to the hydrogen line for the September data, and the solid line in Figure 6*b* shows the range of n_D and b_D permitted by the profile fit to the September deuterium line. The dashed and dotted lines in Figure 6*b* show the range of n_D and b_D consistent with the equivalent width measurements of W_λ(September) = 58 ± 14 mÅ and W_λ(January) = 83 ± 19 mÅ, respectively, which were discussed in § II*b*(ii). We did not apply this detailed profile matching to the January Lα data, because the short-wavelength wing of the hydrogen Lα line is contaminated by geocoronal Lα emission. Best agreement between models and the September data is obtained for $0.10\ \text{cm}^{-3} \leq n_H \leq 0.16\ \text{cm}^{-3}$ and $6\ \text{km s}^{-1} \leq b_H \leq 14\ \text{km s}^{-1}$; but n_H as low as 0.06 cm^{-3} is consistent if $15\ \text{km s}^{-1} \leq b_H \leq 16\ \text{km s}^{-1}$, and n_H as large as 0.20 cm^{-2} is consistent if $4\ \text{km s}^{-1} \leq b_H \leq 6\ \text{km s}^{-1}$. It is possible to fit the hydrogen portion of the profile with values of n_H as low as 0.01 cm^{-3} if $b_H \approx 17$ km s^{-1}; but for these large b_H values, the deuterium line becomes very broad and shallow and it is no longer possible to satisfactorily fit the deuterium profile for any value of n_D/n_H. Examples of very different models of interstellar hydrogen absorption which fit the observed ε Eri profile are given in Figure 7. These models illustrate the sensitivity of the derived value of n_H to the assumed value of b_H for nearby stars, as well as the nonuniqueness of fit when one tries to derive n_H or n_D separately from the Lα profile of one nearby star.

Although it is a reasonable assumption, there is no evidence that the intrinsic stellar profile has the same shape as the solar Lα line. Therefore, additional grids of models were computed using 1. solar profiles with varying amounts and shapes for the self-reversed core of the line, 2. Gaussian-shaped profiles, and 3. flat-topped profiles which were nearly trapezoidal in shape. For the most part, these other profile choices tended to further restrict the range of allowed values shown in Figure 6. The model profiles were found to be particularly insensitive to the amount of self-absorption and shape of the stellar emission lines, and in all cases (including that described in § V*d*), our final choice of intrinsic stellar profile parameters was the one that least constrained the interstellar medium parameters. This insensitivity is understandable, since for the densities observed here the interstellar line is highly saturated over a band ±0.15 Å from line center.

Figure 8 shows a model with $n_H = 0.12$ cm^{-3} and $b_H = 10$ km s^{-1} fitted to the mean January observation. The hydrogen portion of the profile agrees well with the data; however, as noted earlier, the deuterium profile is too narrow.

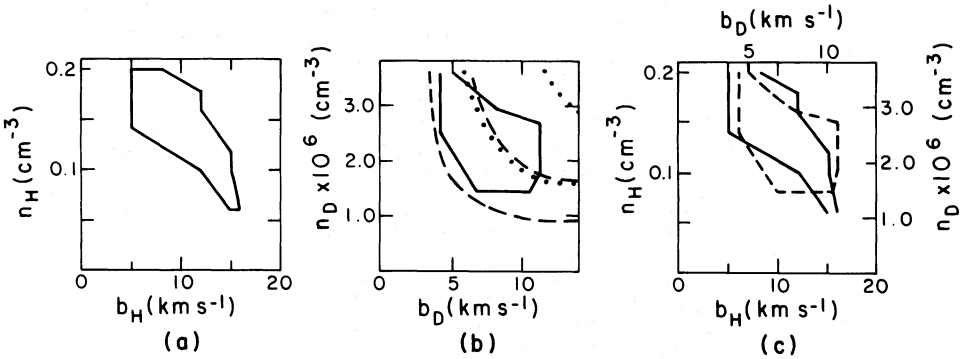

FIG. 6.—The solid line shows (*a*) the allowed range of hydrogen density (n_H) and Doppler dispersion parameter (b_H) derived by fitting model profiles to the September ϵ Eri data, and (*b*) the range of deuterium density (n_D) and Doppler dispersion parameter (b_D) derived by fitting model profiles to the September data. The dashed and dotted lines in Fig. 6*b* show the range of n_D and b_D derived by fitting only equivalent width measurements for the September data and January data, respectively. (*c*) The overlap in the (*dashed line*) deuterium and (*solid line*) hydrogen interstellar parameters assuming $n_D/n_H = 1.8 \times 10^{-5}$ and $b_D/b_H = 1/\sqrt{2}$.

iv) *Multiplication by* exp $[+\tau(\lambda)]$

Profile fitting is not the only method available for analyzing absorption-line data. One may attempt to recover $I_0(\lambda)$ by multiplying the observed profile by exp $[+\tau(\lambda)]$. This technique has been used by a number of authors (e.g., Jenkins 1971; Bohlin 1975) to analyze the Lα line in O and B stars. It works well for hot stars which have a flat continuum; but when the background source is a narrow emission line, the technique may lead to inaccurate results, as the interstellar absorption line is highly saturated. Even for the nearby stars, the optical depth at line center for hydrogen Lα absorption is very large and small errors in the measured values of $I(\lambda)$ are multiplied by large factors near the core of the line (see Bohlin 1975). With high signal-to-noise data the profiles resulting from this multiplication process are still not smooth, particularly near line center, and one must rely on the shape of the far wings in order to determine the continuum level. For dwarf and other stars with narrow emission lines, the stellar profile does not extend far enough beyond the saturated core of the interstellar line to permit an accurate determination of the intrinsic stellar profile by the exp $[+\tau(\lambda)]$ technique. Tests with this method on the ϵ Eri data indicate that the intrinsic profile appears excessively bright (see, for example, the trial profile in Fig. 2 of Dupree *et al.* for $N_H = 3 \times 10^{18}$ cm^{-2}) for values of n_H which are a factor of 3–5 less than the upper limits deduced in our profile fitting (see § IV*b*).

On the other hand, the exp $[+\tau(\lambda)]$ technique may be applied accurately to the less opaque deuterium line, as illustrated in Figure 9. The three curves are reconstructed profiles for deuterium densities 3.9×10^{-6} cm^{-3} ($b_D = 6$ km s^{-1}), 2.2×10^{-6} ($b_D = 8$ km s^{-1}), and 1.3×10^{-6} ($b_D = 12$ km s^{-1}). The middle

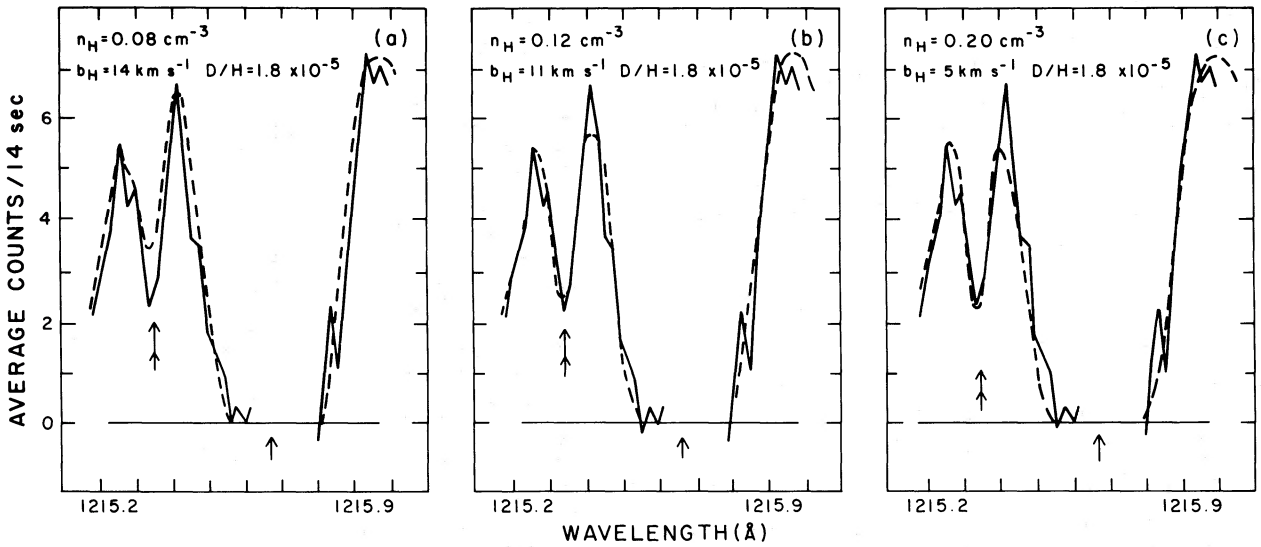

FIG. 7.—Examples of models which fit the September ϵ Eri observation. In (*a*) both the hydrogen and (*dashed line*) deuterium model profiles are nearly too narrow, while in (*c*) both the hydrogen and deuterium profiles are nearly too broad. The parameters $n_H = 0.12$ cm^{-3} and $b_H = 11$ km s^{-1} result in a model shown in (*b*) which fits the data well. Single- and double-headed arrows designate interstellar hydrogen and deuterium line centers, respectively.

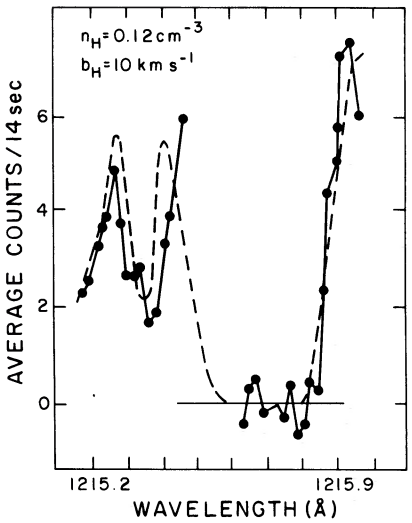

FIG. 8.—Comparison of (*dashed line*) a model profile for $n_H = 0.12\ cm^{-3}$ and $b_H = 10\ km\ s^{-1}$ with (*solid line connecting dots*) the January ϵ Eri observation.

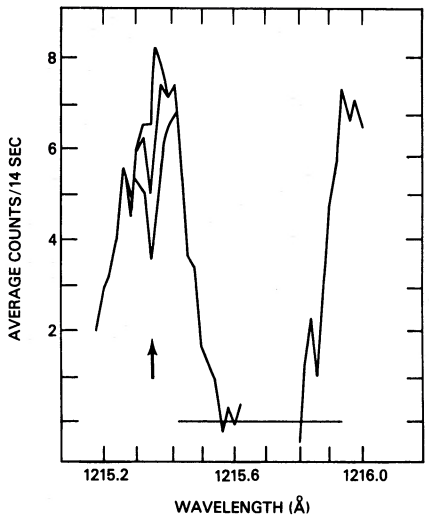

FIG. 9.—The arrow marks examples of intrinsic stellar profiles constructed by multiplying the observed September ϵ Eri profile by exp $(+\tau)$ for deuterium densities of 3.9×10^{-6}, 2.2×10^{-6}, and $1.3 \times 10^{-6}\ cm^{-3}$. In all cases, values of n_D and b_D derived by the multiplication method are consistent with those derived from model fitting. On the other hand, values of n_H derived by this technique were a factor of 3–4 lower than those obtained from the model-fitting procedure.

set of parameters results in an acceptable reconstructed profile, while the other two do not. Values of n_D and b_D deduced from this procedure agree with those found by profile fitting and from measured equivalent widths.

v) *Conclusions*

The curves outlining acceptable ranges of interstellar parameters have been replotted in Figure 6*c* with axes aligned such that $n_D/n_H = 1.8 \times 10^{-5}$, the mean value York and Rogerson (1976) measured toward five OB stars, and $b_H/b_D = \sqrt{2}$. A change in the assumed n_D/n_H ratio corresponds to a shift in the n_D axis in this figure, and a change in the assumed b_H/b_D ratio corresponds to a shift in the b_D axis. If $n_D/n_H = 1.8 \times 10^{-5}$, then the overlap of the deuterium and hydrogen curves restricts n_H to the range 0.08–0.20 cm^{-3} for the September data and the range 0.14–0.20 cm^{-3} for the January data. There is ambiguity in the derived parameters, however, as an increase (decrease) in the assumed n_D/n_H ratio leads to an increase (decrease) in the derived n_H. We consider this problem further in § V.

III. ϵ INDI

Although the distance of ϵ Ind (3.4 pc) is nearly equal to that of ϵ Eri (3.3 pc), the apparent visual brightness of the two stars differs by 1 mag and the total Lα flux from ϵ Ind is a factor of 2 smaller than that from ϵ Eri. The ϵ Ind data are thus of lesser quality. Low-resolution U2 spectra (Fig. 10) were obtained 1976 October 17/18 and consist of 96 scans. We removed particle backgrounds by using U1 as a real-time background monitor.

The solid line in Figure 11 is an average of 48 high-resolution U1 scans of Lα after removal of the particle backgrounds by using the U2 detector as a real-time monitor, and the dashed line is an average of these data after subtraction of backgrounds estimated from the standard table. General agreement between the two subtraction techniques is intermediate to that found for the two ϵ Eri observations. In Figure 11 the thin solid line connecting squares is low-resolution data from Figure 10. Except for a possible relative shift in the wavelength scales, the low- and high-resolution observations are consistent.

We applied a correction of +0.038 Å (+9.3 km s^{-1}) to the U1 wavelengths in Figure 11, using the geocoronal Lα emission as a wavelength standard. This correction is in agreement with the value 9.1 km s^{-1} calculated from the relation of Shull and York (1977). Data points contaminated by geocoronal Lα emission have been deleted from Figures 10 and 11.

The position of the deuterium line center is 1215.45 Å in the rest frame of the star (heliocentric radial velocity, $-39.6\ km\ s^{-1}$),[3] corresponding to a heliocentric velocity of $-12.0 \pm 7.5\ km\ s^{-1}$. The wavelength center of the interstellar hydrogen profile appears to be 1215.75 Å, marked by the single-headed arrow in Figure 11. Although this is 0.03 Å less than the value predicted from the deuterium line center and the isotopic shift of 0.332 Å, the discrepancy is not significant, because the hydrogen absorption profile is substantially blueshifted with respect to the narrow stellar emission feature. Thus, if the intrinsic stellar profile is self-reversed, the blue wing of the observed profile will be lowered in intensity, thereby shifting the center of gravity of the observed interstellar feature toward shorter wavelengths. We there-

[3] This is the mean of the four most recent determinations cited by Abt and Biggs (1972).

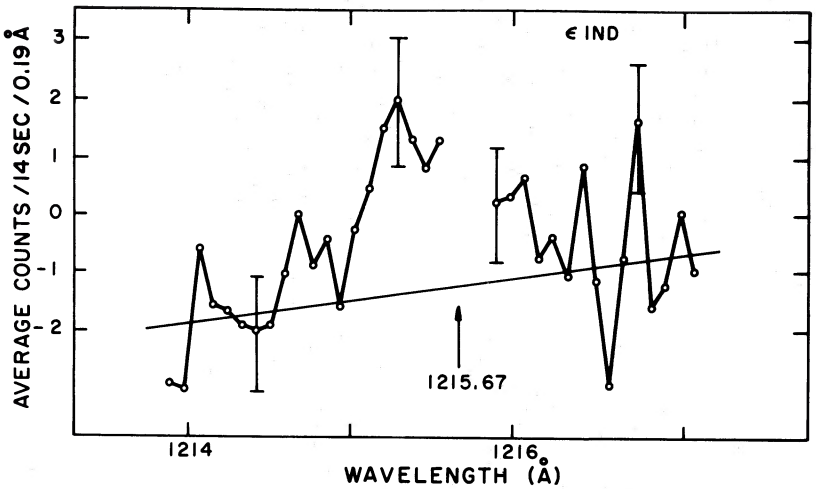

FIG. 10.—The solid line is the low-resolution (U2 ≈ 0.25 Å) profile of the Lα emission line in ϵ Ind. Backgrounds were subtracted using the real-time monitor, and points contaminated by geocoronal Lα emission have been deleted. Error bars refer to ±1 σ errors in the mean.

fore adopt the deuterium wavelength center as a more reliable measurement of the bulk velocity of interstellar material.

Because the data are of poor quality, we did not construct a complete grid of models. The data for this star are, however, consistent with the range of values of n_H and b_H derived for ϵ Eri. The dashed line in Figure 12 is a model profile with $n_H = 0.10\ \mathrm{cm}^{-3}$, $b_H = 11\ \mathrm{km\ s}^{-1}$, and an absorption center blueshifted by 0.11 Å with respect to emission-line center, corresponding to a line-of-sight velocity of -12.0 km s^{-1} for the interstellar material. The intrinsic stellar

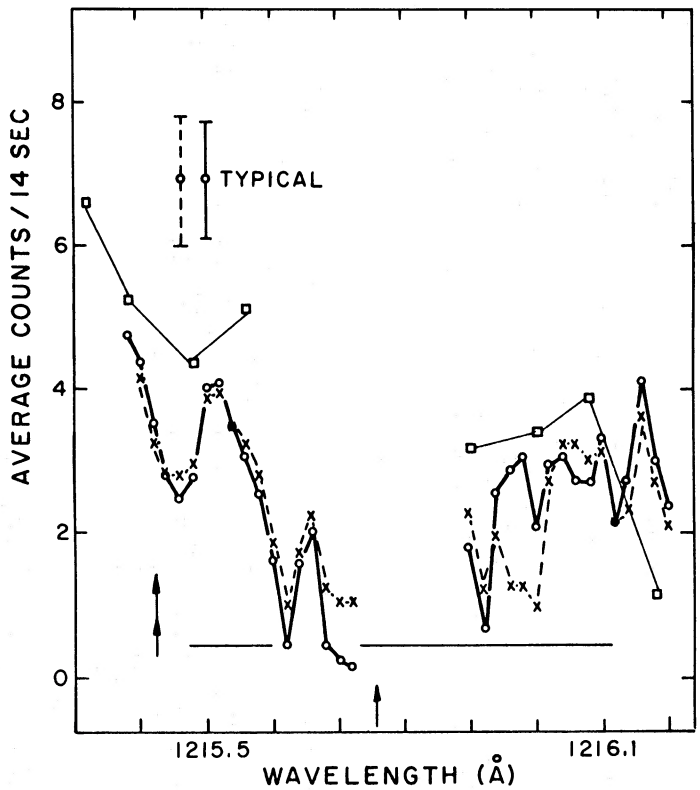

FIG. 11.—The solid line connecting circles is the high-resolution observation of Lα in ϵ Ind after subtraction of a background using the real-time monitor, while the dashed line shows the same initial data but after subtraction of a background estimated from the "standard table." Points contaminated by geocoronal Lα emission are deleted. The thin solid line connecting squares is the low-resolution data from Fig. 10. The single- and double-headed arrows designate interstellar hydrogen and deuterium line centers, and the error bars refer to ±1 σ error in the mean.

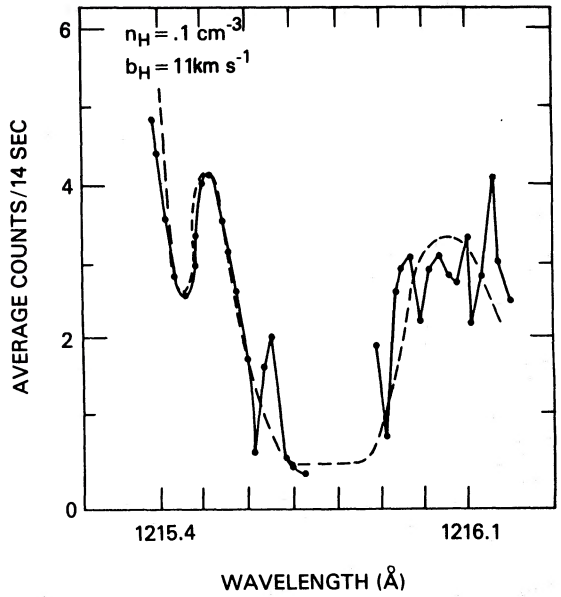

FIG. 12.—Comparison of (*dashed line*) a model profile for $n_H = 0.10\,\mathrm{cm}^{-3}$ and $b_H = 11\,\mathrm{km\,s}^{-1}$ with (*solid line*) the high-resolution observation of ϵ Ind.

profile adopted for this model has a FWHM = 0.8 Å and a 50% self-reversal core. In contrast to ϵ Eri, the degree of self-reversal assumed for the stellar emission line can affect the observed profile. For example, a change from 0% to 100% self-reversal, with all other parameters held fixed, shifts the apparent blue edge of the interstellar absorption 0.18 Å to the blue. This is a consequence of the large difference in radial velocity between the interstellar material and the star.

IV. A REANALYSIS OF *Copernicus* OBSERVATIONS OF α CENTAURI A AND α AURIGAE

Dupree, Baliunas, and Shipman (1977) have recently presented and analyzed *Copernicus* high-resolution Lα spectra of the G2 V star α Cen A and the G5 III + G0 III spectroscopic binary α Aur. These nearby stars, at 1.3 and 14 pc, respectively, constitute important probes of the local interstellar medium. The data were corrected using the standard table of backgrounds, and the interstellar hydrogen and deuterium column densities were derived using the exp $[+\tau(\lambda)]$ method (see § II*b*[iv]) for hydrogen and a curve-fitting technique for deuterium toward α Aur. What is interesting in the results of Dupree *et al.* are the very different values of n_H and n_D/n_H derived for these stars. They derived $n_H = 0.20 \pm 0.05\,\mathrm{cm}^{-3}$ and $n_D/n_H = 0.24 \times 10^{-5}$ for α Cen A, and $n_H = 0.03 \pm 0.01\,\mathrm{cm}^{-3}$ and $n_D/n_H = 3.9 \times 10^{-5}$ for α Aur. If confirmed, these results would require a LISM very inhomogeneous in n_H and, more important, in n_D/n_H (the values for α Cen A and α Aur differ by a factor of 16). To compare these results with our measurements toward ϵ Eri and ϵ Ind, we have reanalyzed these data using the method described in § II.

a) α *Centauri A*

The circles connected by the dashed line in Figure 13 represent the *Copernicus* observation of Lα in α Cen A after subtraction of particle backgrounds estimated from the standard table, while the circles connected by the solid line represent the same data after removal of particle backgrounds by using U2 as a real-time monitor. The overall agreement between the two subtraction techniques is of lesser quality

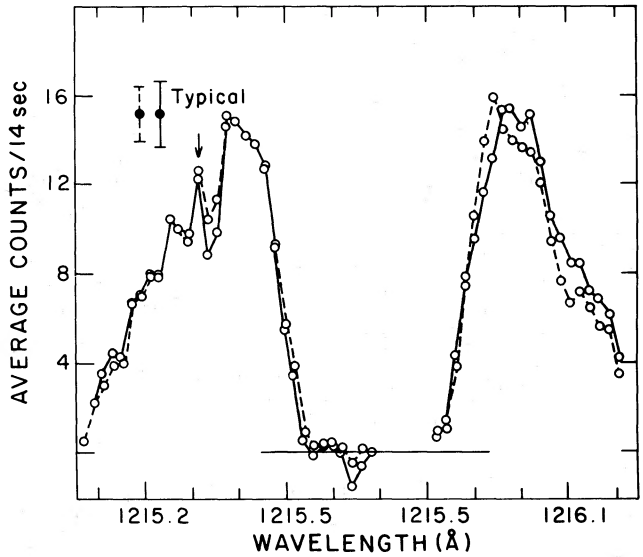

FIG. 13.—The solid line is the high-resolution observation of Lα in α Cen A after subtraction of a background using the real-time monitor. The dashed line shows the same Lα data but after subtraction of a background estimated from the "standard table." Points contaminated by geocoronal Lα emission have been deleted; $\pm 1\,\sigma$ errors in the mean for each data point are noted by the error bars.

than that found for the 1975 September observation of ϵ Eri. Because no *a priori* choice between background subtraction techniques is possible, we adopt the mean of the two curves for comparison with model profiles.

The dashed line in Figure 13 differs slightly from the average shown in Figure 4 of Dupree *et al.*, because we have used a spacing of 0.02 Å between data points to average the 28 separate scans while Dupree *et al.* used a spacing of 0.01 Å. Because the sampling interval of the U1 detector is $\sim$0.02 Å near λ1215, the data points shown in Figure 13 are very nearly statistically independent (although a small correlation is introduced in adjacent data points by the averaging process) while adjacent data points in Figure 4 of Dupree *et al.* are strongly correlated. We note in particular that the "spike" near λ1215.34, marked by an arrow in Figure 13, consists of a single datum, 1 σ above the mean, while in Figure 4 of Dupree *et al.* it appears as at least two data.

Since α Cen A is of the same spectral type as the Sun and has nearly identical chromospheric parameters as determined from the Ca II K line (Ayres *et al.* 1976), we can estimate with reasonable accuracy the intrinsic Lα profile. We assume that the α Cen A profile is the same as the solar profile obtained by Bruner and Rense (1969), with a central intensity 0.67 of the emission peaks, but also consider variants of this profile as we did for ϵ Eri, including a profile 10% wider as suggested by the Ca II K line (Boesgaard and Hagen 1974). Since the solar-type profile allows the widest range of interstellar parameters, its use does not constrain our results.

The solid line in Figure 14 outlines the region in n_H and b_H consistent with the observed α Cen A profile. We find that values of n_H as small as 0.06 cm^{-3} for 14 km s^{-1} < b_H < 16 km s^{-1} and as large as 0.30 cm^{-3} for 10 km s^{-1} < b_H < 14 km s^{-1} are permitted. The reason for this large permitted range in n_H is that the interstellar absorption is at the transition between the flat part and the square-root part of the curve of growth, so that, over a large range of hydrogen column density N_H, one can trade off N_H against b_H and still obtain the same square-well–shaped interstellar absorption profile. This results in part because the saturated portion of the absorption line is quite broad, requiring large b_H (10–15 km s^{-1}) values if an acceptable fit is to be obtained. For these values, the shape of the profile depends strongly on our choice of b_H but only weakly on n_H.

There is a weak feature at 1215.35 Å, which is located at the expected wavelength for interstellar deuterium. However, the line is weak and the data are not of sufficient quality to allow measurement of an accurate equivalent width. We have therefore determined the allowed range of b_D and n_D from the model-fitting procedure alone (§ II*b*). The dashed line in Figure 14 outlines the values of n_D and b_D which are consistent with this analysis. The axes in Figure 14 have been aligned to show the allowed overlap in hydrogen and deuterium densities and *b*-values if $n_D/n_H = 1.8 \times 10^{-5}$ and $b_D/b_H = 1/\sqrt{2}$ (cf. Fig. 6*c*),

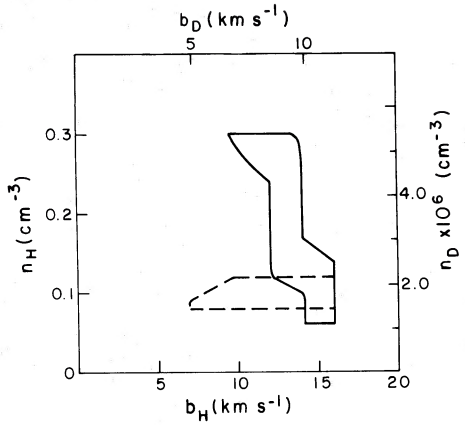

FIG. 14.—The solid line shows (*left-hand ordinate, lower abscissa*) the allowed range of n_H and b_H derived from the model-fitting procedure for α Cen A, while the dashed line shows (*right-hand ordinate, upper abscissa*) the corresponding allowed range of n_D and b_D. The axes of the two plots have been adjusted so that $n_D/n_H = 1.8 \times 10^{-5}$ and $b_D/b_H = 1/\sqrt{2}$.

but these ratios were not assumed in our analysis. We have assumed here and throughout the paper that one velocity is appropriate for both hydrogen and deuterium absorption. If they are not cospatial or if deuterium absorption is primarily in one of several unresolved "clouds," then our estimated range for n_D/n_H can be in error. There is no evidence, however, for this situation.

Examples of profiles for very different interstellar parameters which fit the data are shown in Figure 15. In each plot the observations are shown as circles connected by a solid line. The solid line in Figure 15*a* is a model for $n_H = 0.06$ cm^{-3}, $b_H = 15$ km s^{-1}, and $n_D = 1.4 \times 10^{-6}$ cm^{-3} ($n_D/n_H = 2.4 \times 10^{-5}$). A dashed line shows the profile for $n_H = 0.20$ cm^{-3} and $b_H = 14$ km s^{-1} (identical to the solid line in Fig. 15*c*). This figure dramatically demonstrates the wide range of n_H and b_H allowed by the data. An excellent fit, obtained with a model having $n_H = 0.1$ cm^{-3}, $b_H = 15$ km s^{-1}, and $n_D/n_H = 1.8 \times 10^{-5}$, is shown in Figure 15*b*. Finally, Figure 15*c* compares a model (*solid line*) for $n_H = 0.2$ cm^{-3}, $b_H = 14$ km s^{-1}, and $n_D/n_H = 0.9 \times 10^{-5}$ with a model (*dashed line*) for the interstellar medium parameters derived by Dupree *et al.* ($n_H = 0.2$ cm^{-3}, $b_H = 10$ km s^{-1}, and $n_D/n_H = 0.24 \times 10^{-5}$).

It is important to recognize why we have derived interstellar parameters very different from those obtained by Dupree *et al.* using the same *Copernicus* data. The reasons are the following:

1. For nearby stars there is, in general, a range in values of n_H and b_H which gives nearly identical interstellar absorption profiles, with no *a priori* reason for choosing a unique set of values of these parameters from the hydrogen absorption toward one star.

2. The intrinsic stellar profile derived by Dupree *et al.* for $N_H = 8 \times 10^{17}$ cm^2, corresponding to $n_H = 0.20$ cm^{-3}, does not resemble the solar profile. In particular, the emission peaks are too narrow and the self-reversal too square-well shaped. Their derived

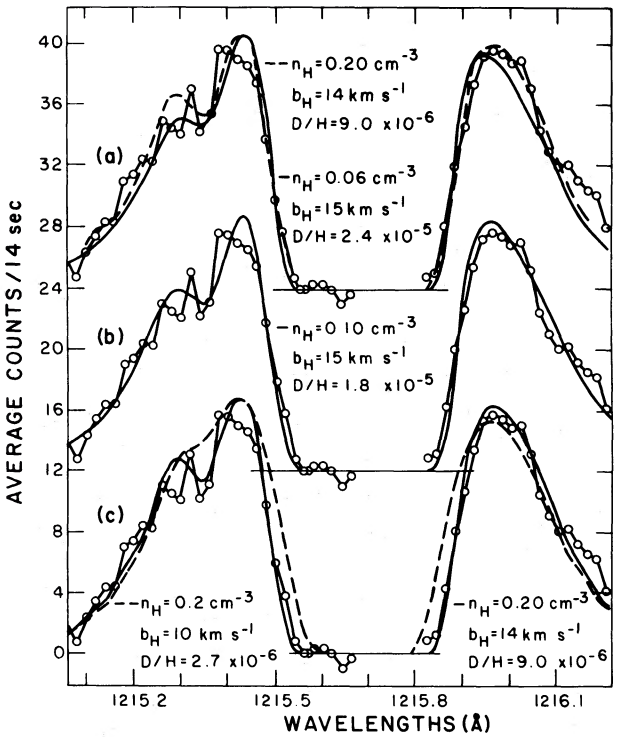

FIG. 15.—Comparison of model profiles with very different interstellar parameters and (*solid line connecting circles*) the high-resolution observations of α Cen A. (*a*) The hydrogen cores of two models with (*dashed line*) $n_H = 0.2\ cm^{-3}$ and (*solid line*) $n_H = 0.06\ cm^{-3}$ are almost indistinguishable, although the model with $n_H = 0.06\ cm^{-3}$ and $n_D/n_H = 2.4 \times 10^{-5}$ better fits the observed deuterium profile than the one with $n_H = 0.20\ cm^{-3}$ and $n_D/n_H = 9.0 \times 10^{-6}$. (*b*) An excellent fit to the data is obtained with $n_H = 0.10\ cm^{-3}$ and $n_D/n_H = 1.8 \times 10^{-5}$. (*c*) Comparison of (*dashed line*) a model profile for the parameters $n_H = 0.20\ cm^{-3}$, $b_H = 10\ km\ s^{-1}$, and $n_D/n_H = 2.7 \times 10^{-6}$ obtained by Dupree *et al.* with (*solid line*) a model profile for the same hydrogen density but larger b_H and deuterium abundance to better fit the hydrogen and the deuterium lines. Note in particular the broad shallow deuterium profile which results from the Dupree *et al.* choice of parameters.

intrinsic stellar profile for $N_H = 8 \times 10^{17}\ cm^{-2}$ has an intensity 0.3 of the emission peaks at $\Delta\lambda = 0.12$ Å from line center, the innermost point they derive. Even this relative intensity is much smaller than observed for the Sun, but there is no assurance that the intrinsic profile closer to line center would not be even deeper if there were less-noisy data with which to derive it. Thus it is not surprising that the parameters $n_H = 0.20 \pm 0.05\ cm^{-3}$ and $b_H = 8$–$10\ km\ s^{-1}$ do not lie within our accepted range in Figure 14.

3. The 10 mÅ deuterium-line equivalent width measured by Dupree *et al.* apparently corresponds to the narrow feature centered at 1215.35 Å with a FWHM = 35 mÅ. The narrowness of this feature is inconsistent with the instrumental resolution (FWHM = 50 mÅ). It is also inconsistent with the large values of b_H derived from the hydrogen profile, since $b_D/b_H \geq 1/\sqrt{2}$ if the two species are cospatial. In fact, if the single data point marked by the arrow in Figure 13 is lowered by 1 σ, much larger half-widths and equivalent widths are indicated. Equivalent widths inferred from our model-fitting procedure range from 30 mÅ ($b_D = 11\ km\ s^{-1}$, $n_D = 2.16 \times 10^{-6}\ cm^{-3}$) to 21 mÅ ($b_D = 5\ km\ s^{-1}$, $n_D = 1.44 \times 10^{-6}\ cm^{-3}$). Even if the line of sight contains an ensemble of velocity components (producing the large derived value of b_H) only one component of which has sufficient column density to produce an observable deuterium feature, the apparent narrowness of the line is still inconsistent with the instrumental profile.

b) α *Aurigae*

The *Copernicus* spectra of α Aur obtained by Dupree *et al.* are of higher signal-to-noise ratio than are those of the other three stars studied here, but the intrinsic stellar profile is difficult to guess *a priori*. Since the star α Aur is a double-line spectroscopic binary, the Doppler-shifted Lα double emission peaks from each star may tend to fill in the line self-reversal from the other star, reducing the composite Lα self-reversal from the system. Indeed, the radial velocities of the primary and secondary are quite different for the two observations: On 1975 February 11/12 (phase[4] ~48 days), V(primary) $\approx 35\ km\ s^{-1}$, whereas on 1976 January 15/16 (phase ~74 days), V(primary) $\approx 4\ km\ s^{-1}$. Despite this large difference in V(primary), the nearly identical line profiles for the two observations suggest that substantial Lα emission originates from both components, unlike the Ca II emission which may be associated only with the primary (Wright 1954). We have therefore included both solar-like profiles and Gaussian profiles in our fitting procedure and have considered a range of self-reversals in the intrinsic profile from total to zero.

The deuterium line is a prominent feature in the α Aur spectrum, but there is some ambiguity in measuring its equivalent width, because the "continuum level" is one wing of a sloping hydrogen absorption line. We estimated this continuum level by fitting our best model as described below (see Fig. 17) but assuming no deuterium. Our value for the equivalent width W_D is 75 ± 5 mÅ, compared to 69.6 ± 2 mÅ (mean of two observations) given by Dupree *et al.* Our major uncertainty arises from the placement of the continuum level.

Figure 16*a* shows the range in values of n_H and b_H derived by model fitting. Our best-fit values $0.04\ cm^{-3} < n_H < 0.05\ cm^{-3}$ are only slightly larger than $n_H = 0.03 \pm 0.01\ cm^{-3}$ derived by Dupree *et al.* The solid line in Figure 16*b* shows the range of n_D and b_D derived by fitting the deuterium profile, while the dashed line delineates the values obtained from the equivalent width measurements. We found that $0.9 \times 10^{-6}\ cm^{-3} \leq n_D \leq 2.5 \times 10^{-6}\ cm^{-3}$ and $5\ km\ s^{-1} \leq b_D \leq 8.5\ km\ s^{-1}$ fitted the data. This range of parameters is similar to the range $0.8 \times 10^{-6}\ cm^{-3} \leq n_D \leq 2.0 \times 10^{-6}\ cm^{-3}$ and $5\ km\ s^{-1} \leq b_D \leq 7\ km\ s^{-1}$ derived by Dupree *et al.*

[4] The orbital elements were taken from Struve and Kilby (1953), with corrections to the zero epoch noted by Wright (1954) and Heintz (1975).

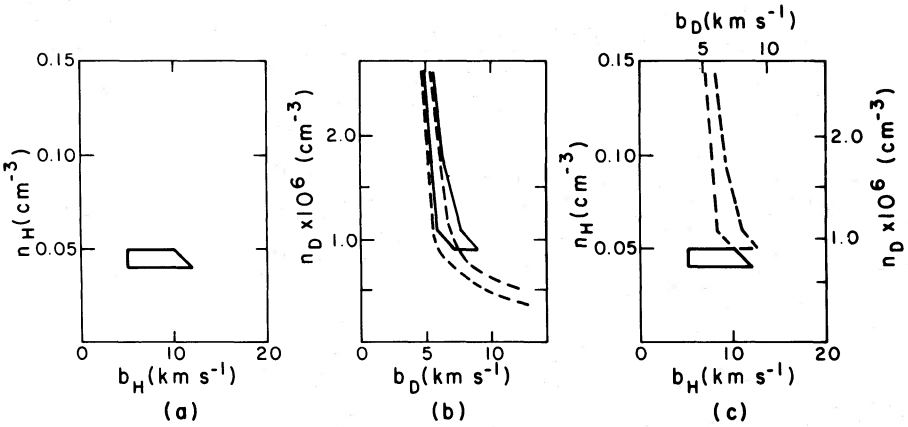

FIG. 16.—The solid line shows (*a*) the range of n_H and b_H derived by fitting model profiles to the α Aur data, and (*b*) the corresponding range of n_D and b_D. The dashed line in Fig. 16*b* shows the range of n_D and b_D derived by fitting only the equivalent width measurements. (*c*) The overlap in the (*dashed line*) deuterium and (*solid line*) hydrogen interstellar parameters assuming $n_D/n_H = 1.8 \times 10^{-5}$ and $b_D/b_H = 1/\sqrt{2}$.

Figure 16*c* shows the allowed (*solid line*) hydrogen parameters and (*dashed line*) deuterium parameters from the model-fitting procedure, with the axes aligned for $n_D/n_H = 1.8 \times 10^{-5}$ and $b_D/b_H = 1/\sqrt{2}$.

Examples of different models are shown in Figure 17. In Figure 17*a* we show our best fit assuming $n_H = 0.05$ cm^{-3}, $b_H = 10$ km s^{-1}, $n_D/n_H = 1.8 \times 10^{-5}$, and $b_D = 7$ km s^{-1}. The dashed line is a profile assuming $n_D = 0$ cm^{-3}, which was used to compute the deuterium Lα equivalent width. A second model with the same hydrogen parameters but with $n_D/n_H = 3.6 \times 10^{-5}$ and $b_D = 5$ km s^{-1} is shown in Figure 17*b*. Comparison of these two profiles dramatically illustrates the large range of n_D consistent with the data. Finally, Figure 17*c* shows the computed profile using the parameters derived by Dupree *et al.*: $n_H = 0.03$ cm^{-3}, $b_H = 10$ km s^{-1}, $n_D = 1.1 \times 10^{-6}$ cm^{-3} ($n_D/n_H = 3.9 \times 10^{-5}$), and $b_D = 8$ km s^{-1}. In general, the best agreement between the models and the data was obtained using intrinsic profiles with Gaussian wings for $0.04 \text{ cm}^{-3} \leq n_H \leq 0.05 \text{ cm}^{-3}$. The model shown in Figure 17*c* was computed using a solar-like profile and a 50% self-absorption in accordance with the assumptions made by Dupree *et al.* For both Gaussian and solar-like profiles with up to 50% self-absorption, we found no detectable difference in the computed profiles.

c) *Conclusion*

We find a slightly larger range of hydrogen densities ($0.06 \text{ cm}^{-3} \leq n_H \leq 0.30 \text{ cm}^{-3}$) and a considerably higher range of *b*-values ($10 \text{ km s}^{-1} \leq b_H \leq 16$ km s^{-1}) for the α Cen data than the ranges quoted by Dupree *et al.* ($0.15 \text{ cm}^{-3} \leq n_H \leq 0.25 \text{ cm}^{-3}$ and $8 \text{ km s}^{-1} \leq b_H \leq 10 \text{ km s}^{-1}$). Our deuterium densities toward α Cen ($1.4 \times 10^{-6} \text{ cm}^{-3} \leq n_D \leq 2.2 \times 10^{-6} \text{ cm}^{-3}$) are about a factor of 4 larger than those of Dupree *et al.* ($0.42 \times 10^{-6} \text{ cm}^{-3} \leq n_D \leq 0.55 \times 10^{-6} \text{ cm}^{-3}$). We ascribe this discrepancy chiefly to what we feel is their underestimated equivalent width of 10 mÅ for the deuterium line due to their interpretation of a single datum which is 1 σ above the true mean value. In § V we discuss the limits on the n_D/n_H ratio which are consistent with these data and with the data for ϵ Eri and ϵ Ind.

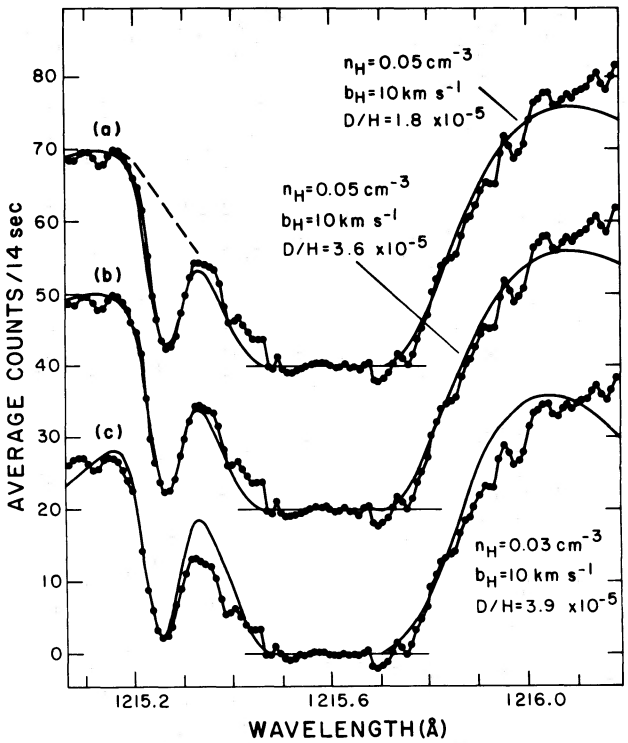

FIG. 17.—Comparison of model profiles with different interstellar parameters and (*solid line connecting filled circles*) the high-resolution observations of α Aur. Model profiles in (*a*) and (*b*) have the same $n_H = 0.05$ cm^{-3}, but n_D differs by a factor of 2 from (*a*) $n_D/n_H = 1.8 \times 10^{-5}$ and $b_D = 7$ km s^{-1} to (*b*) $n_D/n_H = 3.6 \times 10^{-5}$ and $b_D = 5$ km s^{-1}. (*c*) A comparison of a model with $n_H = 0.03$ cm^{-3} and $n_D/n_H = 3.9 \times 10^{-5}$ (Dupree *et al.*), and the data.

V. DISCUSSION

Properties of the neutral hydrogen component of the LISM have now been estimated using three observational techniques: Lα and Mg II *h* and *k* line absorption toward the nearest hot stars, Lα absorption toward nearby cool stars, and solar Lα and He I λ584 backscattering experiments.

The three observational techniques sample different regions of space. For A-type stars the stellar Lα line is in absorption and is very broad, providing a poor source against which to measure interstellar absorption. For this reason most of the observational studies of the LISM have used as sources O and early B stars, which have narrow stellar Lα lines. Since the nearest B star, α Leo (B7 V), is 22 pc distant, this technique can yield only spatial averages over at least this path length. In fact, hotter stars should be used in this work, and η UMa (B3 V) at 41 pc is perhaps the nearest useful star. Recently, Kondo *et al.* (1978) reported measurements of Mg II column densities and b_{Mg} values toward four nearby stars: α CMa ($d = 2.67$ pc), α Lyr ($d = 8.13$ pc), α Gru ($d = 19.6$ pc), and α Leo ($d = 25.6$ pc). Although these results cannot be used to infer hydrogen column densities because the degree of magnesium depletion with respect to hydrogen toward these stars (e.g., Spitzer and Jenkins 1975) is unknown and may be variable (Snow 1975; Hobbs 1975), the line-of-sight bulk velocities may be used to probe the macroscopic motion of the gas.

Cool stars with Lα in emission are useful background sources only when their weak Lα emission is observable and when the interstellar absorption is significantly narrower than the stellar Lα emission line. The useful region of space that has been sampled in this way is 1.33 pc (α Cen) to about 21 pc (α Tau); but, as noted above, this method is most useful for stars within 10 pc.

By contrast, the Lα and He I λ584 backscattering experiments sample only the LISM flowing through the solar system out to about 100 AU (0.0005 pc).

a) LISM Properties in the Line of Sight to Cool Stars

Interstellar hydrogen and deuterium absorptions have been measured toward eight nearby stars using *Copernicus* Lα spectra. These data are summarized in Table 1. Included in the table are the galactic coordinates, the distance to each star, and the derived range of hydrogen and deuterium densities and *b*-values. Also given are the stellar radial velocity (V_r), the line-of-sight velocity (LOSV) of the local standard of rest (V_{LSR}), the LOSV of the neutral hydrogen which flows into the solar system (V_{HI}), and the observed LOSV derived from the *Copernicus* spectra (V_0). In the case of two of these stars, α Tau and β Gem, only U2 (0.25 Å) resolution observations are available and the hydrogen densities derived from these data are tentative. In the case of α Boo, high-quality, high-resolution observations exist, but ambiguities in these data permit the determination of only an upper limit $n_H < 0.15\ cm^{-3}$ toward this star (McClintock *et al.* 1978, Paper VI).

Except for the deuterium density toward α Cen A, our measurements of densities and *b*-values are in reasonable agreement with those of Dupree *et al.*; but our conclusions regarding the local deuterium-to-hydrogen ratio are quite different. In each case, a large range of n_D/n_H is allowed by the data (see Figs. 6, 14, and 16). This ambiguity in the present data arises partly from the low signal-to-noise ratio (except for α Aur) and partly from the nonuniqueness in selecting a single *b*-value and density (note the large range of n_D versus b_D for α Aur). We believe that Dupree *et al.* have not pointed out the large range of interstellar parameters consistent with their data and have misinterpreted their deuterium observations toward α Cen A, which may be in error because of the low signal-to-noise ratio in the data. We note that the b_{Mg} values obtained by Kondo *et al.* (1978) are in the range 4.9–5.9 km s^{-1}. If these broadening velocities arise purely from thermal motions, the corresponding b_H value will be ~32 km s^{-1}, suggesting that part of the dispersion is turbulent rather than thermal. The b_H/b_D ratio is not well determined in our analysis, but it should lie between 1 and $\sqrt{2}$. If $b_H/b_D < \sqrt{2}$, the dashed curves in Figures 6*c*, 14, and 16*c* would be compressed to the left by a factor less than $\sqrt{2}$; however, none of our conclusions would be altered.

b) Comparison with Hydrogen and Helium Backscatter Results

The physical parameters of the very local ($d \lesssim 5 \times 10^{-4}$ pc) interstellar medium have been estimated by observing the intensities of resonantly scattered solar hydrogen and helium radiation by atoms in interplanetary space. Extensive sky maps of Lα and He I λ584 emission (for reviews, see Fahr 1974; Thomas 1978) have led to determinations of the density, temperature, and direction of the "interstellar wind" which penetrates the solar system. Direct measurements of the inflow velocity $V = 21.6 \pm 2.8$ km s^{-1} have been made by Adams and Frisch (1977).

To summarize the current picture briefly, the interstellar gas appears to approach the solar system from a direction $\alpha = 252° \pm 3°$, $\delta = -15° \pm 3°$. This direction, based on He I λ584 sky maps of Weller and Meier (1974), is likely to be more precise than the direction $\alpha = 263°$, $\delta = -23°$ determined from the Lα data (Thomas 1978). This vector is different from the motion of the solar system with respect to nearby stars (20 km s^{-1} in the direction $\alpha = 268°$, $\delta = 30°$ [Allen 1973]). Thus the local gas and the nearby stars have their own peculiar motions. The present observational evidence suggests $T \approx 10^4$ K and $0.05\ cm^{-3} \leq n_H \leq 0.10\ cm^{-3}$ (Thomas 1978) for the local interstellar material; an inflow velocity $V = 22$ km s^{-1} (Adams and Frisch 1977); and a direction $\alpha = 252°$, $\delta = -15°$ ($b^{II} = 4°$, $l^{II} = 16°$) (Weller and Meier 1974).

The density and temperature (10^4 K corresponds to $b_H \approx 13$ km s^{-1}) derived from the backscatter measurements are in good agreement with the present

TABLE 1

SUMMARY OF RESULTS

Star	Sp. Type	l^{II}	b^{II}	d (pc)	n_H (cm^{-3})	b_H (km s^{-1})	$n_D \times 10^{+6}$ (cm^{-3})	b_D (km s^{-1})	$(n_D/n_H) \times 10^5$	V_r	V_{LSR}	$V_{H\,I}$	V_0	Ref.
α Cen A...	G2 V	316	−1	1.33	0.15–0.25	8–10	0.42–0.53	...	0.24	−22	...	...	−10.3 ± 7	6
					0.06–0.30	10–16	1.4–2.2	5–11	...	...	+3.6	−6.6	...	10
					0.10–0.20*	13–15*	1.8–2.0*	10–11*	0.9–2.0	...	...	...	...	
ε Eri.....	K2 V	196	−48	3.3	0.01–0.10†	...	...	...	...	+15.4	...	...	...	3
					0.04–0.12	6–16	Present	...	...	...	...	...	...	4
					0.06–0.20	4–18	1.4–3.6	4–11	...	...	+12.0	+17.2	+17.9 ± 7.5	10
					0.10–0.16*	6–14*	1.8–2.9*	5–9*	1.1–2.9	...	...	...	...	
ε Ind.....	K5 V	336	−48	3.4	~0.1	~11	~2	~8	~1.8	−39.6	+3.3	−6.7	−12.0 ± 7.5	10
α CMi.....	F5 IV–V	214	+13	3.5	0.015–0.03†	...	...	...	1.0–2.0	−3	...	...	...	7
					0.09–0.13	9–14	...	...	0.7–1.9	...	+14.8	+14.7	+17 ± 7.5	8
β Gem.....	K0 III	192	+23	10.8	0.02–0.15†	...	...	...	...	+3	+9.2	+14.7	...	1
α Boo.....	K2 IIIp	15	+69	11.1	0.02–0.15†	...	...	...	...	−5	−11.9	−12.5	...	1
					< 0.15	...	...	...	...	...	...	...	...	2
α Aur.....	G5 III + G0 III	163	+5	14.1	< 0.01†	...	...	...	...	...	...	...	...	5
					0.02–0.04	(10)	0.8–2.0	5–7	3.9	+29	...	...	+24.1 ± 7.5	6
					0.04–0.05	5–12	0.9–2.5	5–9	...	...	...	...	...	10
					0.05*	8–10*	0.9–2.0*	6–8*	1.8–4.0	...	+4.5	+17.1	...	
α Tau.....	K5 III	181	−20	20.8	0.02–0.15†	...	...	...	...	+54	...	...	...	1
α CMa.....	A1 V	227	−9	2.67	...	...	...	...	...	−8	+18.3	+15.9	+10.5 ± 7	9
α Lyr.....	A0 V	39	+7	8.13	...	...	...	...	...	−14	−19.8	−11.0	−22.4 ± 7	9
α Gru.....	B7 IV	350	−52	19.6	...	...	...	...	...	+12	+2.1	−6.7	−11 ± 7	9
α Leo.....	B7 V	226	+49	25.6	...	...	...	...	...	+4	+4.3	+4.9	+6.6 ± 7	9

* Best-fit values.

† Hydrogen densities derived from low-resolution (U2) *Copernicus* spectra.

REFERENCES.—(1) Paper III. (2) Paper VI. (3) Paper IV. (4) Paper V. (5) Dupree 1975. (6) Dupree *et al.* 1977. (7) Evans *et al.* 1975. (8) Anderson *et al.* 1978. (9) Kondo *et al.* 1978. (10) Present work.

work for the four closest stars (1.33 pc $\leq d \leq$ 3.5 pc), which suggests $n_H \approx 0.1$ cm^{-3} and $b_H \approx 11$ km s^{-1}. An exception may be α Cen A, for which $b \approx 15$ km s^{-1}, corresponding to a somewhat higher temperature ($T \approx 13{,}000$ K) or turbulence. On the other hand, the average density $n_H \approx 0.04$–0.05 cm^{-3} toward α Aur appears to be a factor of 2 less than for the nearest stars.

If the material in the upwind direction were characteristic of the LISM in general, one would expect the interstellar absorption lines toward nearby stars to have heliocentric velocities corresponding to the components of the interstellar wind velocity of Adams and Frisch projected along the various lines of sight. These velocities are given as V_{HI} in Table 1. Also included in Table 1 are the line-of-sight velocities of the local standard of rest V_{LSR} and the heliocentric velocities of the Mg II absorption lines measured by Kondo *et al.* (1978). With the exception of α Lyr, the observed heliocentric velocities V_0 more closely correlate with V_{HI} than with V_{LSR}. *Therefore, our present results suggest that the very local gas flowing into the solar system may fill the line of sight to the four nearest stars, but the low column density toward α Aur suggests that this material may extend to only 3.5 pc in that direction.* The material in the remaining line of sight toward α Aur appears to have the same velocity but much lower density.

c) *An Emerging Picture of the Nearby Interstellar Medium*

There is now considerable evidence that the properties of interstellar matter along lines of sight to nearby O–B stars like λ Sco (York 1974), α Vir, λ Sco, and β Cen (York 1976) are quite complex. Recent analyses of the multicomponent ultraviolet absorption line profiles toward μ Col and HD 28497 (Shull and York 1977) and toward HD 50896 (Shull 1977) indicate that most of the neutral hydrogen in these lines of sight (468–1500 pc) is concentrated in clouds with $n_H > 10^2$ cm^{-3} and dimensions less than 0.05 pc in some cases. Also, $n_H < 0.01$ cm^{-3} has been derived toward some stars, including the high-galactic-latitude star HZ 43 (63 pc) by Auer and Shipman (1977) and β CMa (213 pc) and ϵ CMa (179 pc) by Bohlin (1975). These results suggest that the density of the interstellar medium is highly variable over scales large compared to the distance of the stars we have studied.

Since individual condensations with distinct velocities and scale lengths $\sim$0.05 pc exist over longer path lengths, one might expect, over path lengths of 1.3–14 pc, the appearance of such clouds as distinct velocity components toward the four stars we have studied. However, we see no direct evidence for multiple components. We must point out that, if there are unresolved clouds with velocity differences $\sim\frac{1}{2}$ our derived value of b_H, then the mean density of the LISM along the lines of sight toward the stars under study could be much lower than stated here.

In summary, we find that the data are consistent with a region extending out to at least 3.5 pc from the Sun, for which the LISM is relatively homogeneous. For the sample of these stars we have analyzed (ϵ Eri, ϵ Ind, and α Cen A), for α CMi (Anderson *et al.* 1978), and for the solar system, the data are all consistent with $n_H \approx 0.10$ cm^{-3} and a flow velocity of 22 km s^{-1} from the direction $\alpha = 252°$, $\delta = -15°$. Within this region the observations are all consistent with $b_H \approx 11$ km s^{-1}, corresponding to $T = 7350$ K if the broadening is entirely thermal, except that $b_H \approx 15$ km s^{-1} toward α Cen A. Beyond 3.5 pc, $n_H = 0.04$–0.05 cm^{-3} toward α Aur (14 pc), but the vector flow of interstellar hydrogen is consistent with the local flow on this line of sight. We also find no conclusive evidence that the deuterium-to-hydrogen ratio within 14 pc of the Sun is significantly different from the value $1.8 \pm 0.4 \times 10^{-5}$ derived by York and Rogerson (1976) for stars at 81 pc $< d <$ 1000 pc. We are currently observing 10 G–K dwarf stars with $d < 10$ pc in order to assess further the degree of homogeneity of n_H and b_H in the LISM, and to investigate the local n_D/n_H ratio.

d) *A Reexamination of the Local Interstellar Cloud Hypothesis of Vidal-Madjar et al.*

Vidal-Madjar *et al.* (1978) have proposed that an interstellar cloud in the direction of the Sco-Oph association "is approaching the solar system from a distance of about 0.03 pc at a velocity of 15–20 km s^{-1}," implying that the solar system will be embedded in this cloud in only 10^4 years. The authors point out some interesting implications of such an encounter; in particular, they note that important changes in the terrestrial climate, such as the onset of an ice age, may occur. In view of the great importance that major changes in the terrestrial climate would have, the Vidal-Madjar *et al.* paper, and the data upon which it is based, must be critically assessed in order to judge the plausibility of their "local interstellar cloud" hypothesis.

They present the following three pieces of evidence for the existence of the local cloud: (1) Evidence for a strong gradient in the hydrogen density in the local interstellar medium. (2) Evidence for an anisotropy in the local ultraviolet flux. (3) Evidence for a significant difference in the deuterium-to-hydrogen ratio between the lines of sight toward α Cen A and α Aur.

We will not comment here on the methods by which Vidal-Madjar *et al.* derived the properties of their proposed local interstellar cloud from these three sets of data. It is sufficient to say that, if the data are not correct, then neither is their conclusion.

As previously noted, good-quality, high-spectral-resolution Lα profiles obtained with the U1 channel of *Copernicus* are now available for four late-type stars: α CMi (F5 IV–V) (Anderson *et al.* 1978), α Cen A (G2 V) and α Aur (G5 III + G0 III) (Dupree *et al.*), and ϵ Eri (K2 V) (Paper VI). The Dupree *et al.* results (see § IV) imply that the hydrogen density toward α Aur is 0.15 times that toward α Cen A and the n_D/n_H ratio toward α Aur is 16 times that toward α Cen A. These ratios, together with the commonly

cited value $n_H = 0.05$–$0.10\ cm^{-3}$ for the density of interstellar hydrogen flowing through the solar system (e.g., Adams and Frisch 1977; Ajello 1978), form the primary basis for points (1) and (3) cited above.

We have shown in Figures 6, 14, and 16 that, for nearby stars, there is a trade-off between N_H and b_H such that nearly identical computed profiles can result from large values of N_H with small values of b_H or the reverse. Thus a wide range of N_H is consistent with the data. A similar trade-off between N_D and b_D results in nearly identical computed profiles. Anderson *et al.* (1978) find such trade-off in values of N_H, b_H and N_D, b_D in their profile-synthesis study of α CMi.

We now consider whether all of these data warrant points (1) and (3). In Figures 7*b*, 15*b*, and 17*a* we compare observed profiles for the four stars with theoretical profiles computed for $n_D/n_H = 1.8 \times 10^{-5}$ and $n_H \approx 0.10\ cm^{-3}$, except that $n_H = 0.05\ cm^{-3}$ for α Aur, and $b_D/b_H = 1/\sqrt{2}$.

Our purpose is not to "prove" homogeneity of the local interstellar medium. Indeed, given the trade-offs described above, it is not possible at this time to verify homogeneity. Instead, we point out that the data *are consistent with* a constant value of n_D/n_H for all four stars and $n_H \approx 0.10\ cm^{-3}$ for the solar system and the three stars within 3.5 pc. As a result, we feel that point (3) is not substantiated and that point (1) is not substantiated for stars within 3.5 pc.

An additional point is that, for eight of the nine stars listed in Table 1 for which there are good data, the measured line-of-sight interstellar flow velocities (V_0) are consistent with uniform flow in all lines of sight out to 25.6 pc. Thus no "cloud" is evident in the local interstellar flow pattern.

We agree with point (2), that there is probably an anisotropy in the local far-ultraviolet flux (Henry 1977). Vidal-Madjar *et al.* (1978) propose that deuterium can be separated from hydrogen by means of the radiation pressure due to this anisotropy of the local ultraviolet flux. However, they explicitly point out that this mechanism can operate only in the presence of a density gradient in the LISM (point [1]). Since there appears to be no strong evidence for the latter within 3.5 pc, the radiation pressure mechanism is not applicable.

We conclude that the "local cloud" hypothesis is an interesting but unsupported speculation, and that it is premature to begin planning for any climatic changes that might be associated with the penetration of such a cloud into the solar system in 10^4 years.

This work was supported by the National Aeronautics and Space Administration under grants NGR-06-003-057 and NAS 5-23274 to the University of Colorado and NSG 5078 to the Johns Hopkins University. We thank R. C. Anderson for a portion of the data reduction, and the referee for a most careful and thoughtful critique of the paper. We also thank Dr. Vidal-Madjar for sending us a preprint of his paper and his comments, and Dr. Dupree for her comments.

REFERENCES

Abt, H. A., and Biggs, E. J. 1972, *A Bibliography of Stellar Radial Velocities* (Tucson: Kitt Peak National Observatory).
Adams, T. F., and Frisch, P. C. 1977, *Ap. J.*, **212**, 300.
Ajello, J. M. 1978, *Ap. J.*, **222**, 1068.
Allen, C. W. 1973, *Astrophysical Quantities* (3d ed.; London: Athlone Press).
Anderson, R., Henry, R. C., Moos, H. W., and Linsky, J. L. 1978, *Ap. J.*, **226**, in press.
Auer, L. H., and Shipman, H. L. 1977, *Ap. J. (Letters)*, **211**, L103.
Ayres, T. R., Linsky, J. L., Rodgers, A. W., and Kurucz, R. L. 1976, *Ap. J.*, **210**, 199.
Boesgaard, A. M., and Hagen, W. 1974, *Ap. J.*, **189**, 85.
Bohlin, R. C. 1975, *Ap. J.*, **200**, 402.
Bruner, E. C., Jr., and Rense, W. A. 1969, *Ap. J.*, **157**, 417.
Dupree, A. K. 1975, *Ap. J. (Letters)*, **200**, L27.
Dupree, A. K., Baliunas, S. L., and Shipman, H. L. 1977, *Ap. J.*, **218**, 361.
Evans, R. G., Jordan, C., and Wilson, R. 1975, *Nature*, **253**, 612.
Fahr, H. J. 1974, *Space Sci. Rev.*, **15**, 482.
Gerola, H., Linsky, J. L., Shine, R. A., McClintock, W., Henry, R. C., and Moos, H. W. 1977, *Ap. J. (Letters)*, **218**, L32.
Heintz, W. D. 1975, *Ap. J.*, **195**, 411.
Henry, R. C. 1977, *Ap. J. Suppl.*, **33**, 451.
Hobbs, L. M. 1975, *Ap. J.*, **202**, 628.
Jenkins, E. B. 1971, *Ap. J.*, **169**, 25.
Kelch, W. L. 1978, *Ap. J.*, **222**, 931.
Kondo, Y., Talent, D. L., Barker, E. S., Dufour, R. J., and Modisette, J. L. 1978, *Ap. J. (Letters)*, **220**, L97.
McClintock, W. 1977, Ph.D. thesis, the Johns Hopkins University.
McClintock, W., Henry, R. C., Moos, H. W., and Linsky, J. L. 1975*a*, *Ap. J.*, **202**, 733 (Paper IV).
———. 1976*a*, *Ap. J. (Letters)*, **204**, L103 (Paper V).
———. 1976*b*, *Bull. AAS*, **7**, 547.
McClintock, W., Linsky, J. L., Henry, R. C., Moos, H. W., and Gerola, H. 1975*b*, *Ap. J.*, **202**, 165 (Paper III).
McClintock, W., Moos, H. W., Henry, R. C., Linsky, J. L., and Barker, J. S. 1978, *Ap. J. Suppl.*, **37**, 223 (Paper VI).
Münch, G. 1968, in *Nebulae and Interstellar Matter*, ed. B. M. Middlehurst and L. H. Aller (Chicago: University of Chicago Press), p. 365.
Nachman, P., and Hobbs, L. M. 1973, *Ap. J.*, **182**, 481.
Shull, M. J. 1977, *Ap. J.*, **212**, 102.
Shull, M. J., and York, D. G. 1977, *Ap. J.*, **211**, 803.
Snow, T. P. 1975, *Ap. J. (Letters)*, **202**, L87.
Spitzer, L., and Jenkins, E. B. 1975, *Ann. Rev. Astr. Ap.*, **13**, 133.
Struve, O., and Kilby, R. 1953, *Ap. J.*, **117**, 272.
Thomas, G. E. 1978, *Ann. Rev. Earth Planet. Sci.*, **6**, in press.
Vidal-Madjar, A., Laurent, C., Bruston, P., and Audouze, J. 1978, *Ap. J.*, **223**, 589.
Weller, C. S., and Meier, R. R. 1974, *Ap. J.*, **193**, 471.
Wright, K. O. 1954, *Pub. Dom. Ap. Obs.*, **10**, 1.
York, D. G. 1974, *Ap. J. (Letters)*, **193**, L127.
———. 1976, *Ap. J.*, **204**, 750.
York, D. G., and Rogerson, J. B. 1976, *Ap. J.*, **203**, 378.

R. C. HENRY: Code SC, National Aeronautics and Space Administration, Washington, DC 20546
J. L. LINSKY: Joint Institute for Laboratory Astrophysics, University of Colorado, Boulder, CO 80309
W. MCCLINTOCK: Laboratory for Atmospheric and Space Physics, University of Colorado, Boulder, CO 80309
H. W. MOOS: Physics Department, The Johns Hopkins University, Baltimore, MD 21218